Earthquake Geotechnical Engineering, Sêco e Pinto (ed.) © *1999 Balkema, Rotterdam, ISBN 90 5809 116 3*

Permanent strain and pore pressure relations for cyclic loading of sand

D.N.Egglezos & G.D.Bouckovalas
National Technical University of Athens, Greece

ABSTRACT: A set of empirical relations is developed for the prediction of permanent shear strain and excess pore pressure accumulation during undrained, cyclic triaxial loading of sand. For this purpose, a multi-variable regression analysis is performed on results from 179 isotropic and anisotropic tests, using as variables the initial stresses, the cyclic shear stress amplitude, the volume density and the applied number of load cycles. The relations provide the means for simplified computations of settlements and bearing capacity of foundations. In addition, they can be used as reference for the calibration of constitutive models aimed at the prediction of cyclic sand response.

1 INTRODUCTION

Cyclic loading of cohesionless materials, at moderate and large shear stress or strain amplitudes, is known to cause accumulation of permanent strain and excess pore pressure build up. As a results, foundations may accumulate settlements or undergo bearing capacity degradation, retaining structures may sustain increased lateral pressures, while sloping grounds may develop lateral spreading.

A thorough geotechnical analysis of the above cases, presumes the use of appropriate numerical codes, as well as soil models that can predict with accuracy the plastic response of soil elements under repetitive loading. However, there are cases where alternative, simplified means of analysis may be preferable, e.g during preliminary computations or when the lack of the necessary soil parameters and the appropriate constitutive models for cyclic loading prevent the use of numerical codes. It should be reminded that this practice is rather common in geotechnics. For instance, consolidation settlements are most often assessed from one dimensional, hand computations instead from more strict three dimensional numerical analyses.

In the following, a set of empirical relations is developed for the computation of permanent shear strains and excess pore pressures in sands subjected to cyclic loading. Namely, a statistical analysis is performed on results from 104 isotropic and 63 anisotropic undrained cyclic triaxial tests in order to determine the effects of initial stress conditions, cyclic shear stress amplitude, volume density and number of load cycles. In addition to the means for

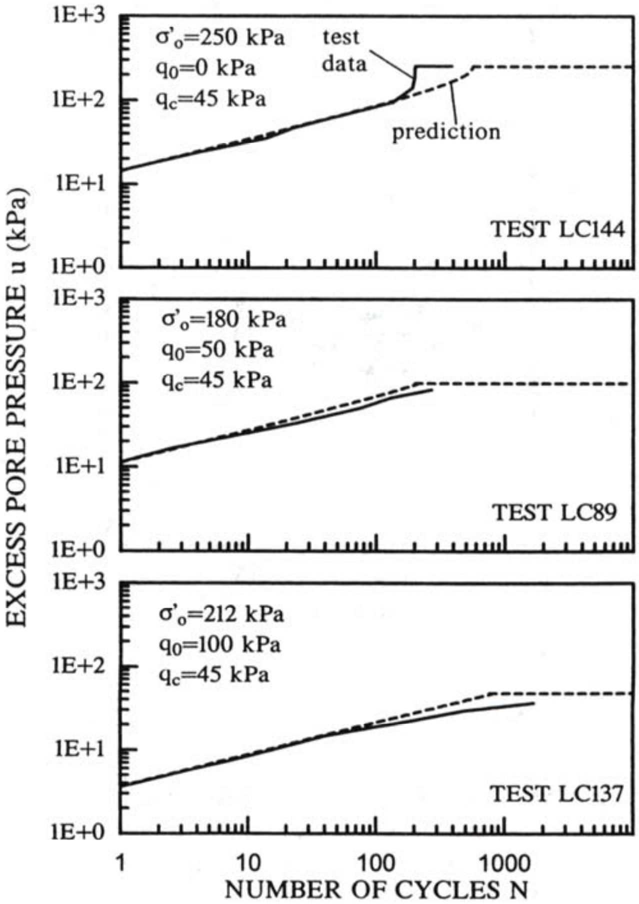

Figure 1. Typical experimental data for the variation of excess pore pressure with number of cycles (Oosterschelde sand).

Table 1. Range of stress conditions in the analyzed undrained cyclic triaxial tests

	Relations for Excess Pore Pressure		Relations for Permanent Shear Strain	
	Oosterschelde Sand	NTUA Sand	Oosterschelde Sand	NTUA Sand
No. of tests	75	102	43	14
q_c/σ'_o	0.07 - 0.43	0.06 - 0.61	0.08 - 0.35	0.14 - 0.40
σ'_o/p_a	0.42 - 7.00	0.29 - 3.28	0.42 - 6.47	1.48 - 1.63
Q	0.00 - 0.89	0.06 - 1.10	0.17 - 1.01	0.28 - 1.10
q_o/q_c	0.00 - 5.00	0.0 - 3.06	0.91 - 3.33	0.47 - 3.37

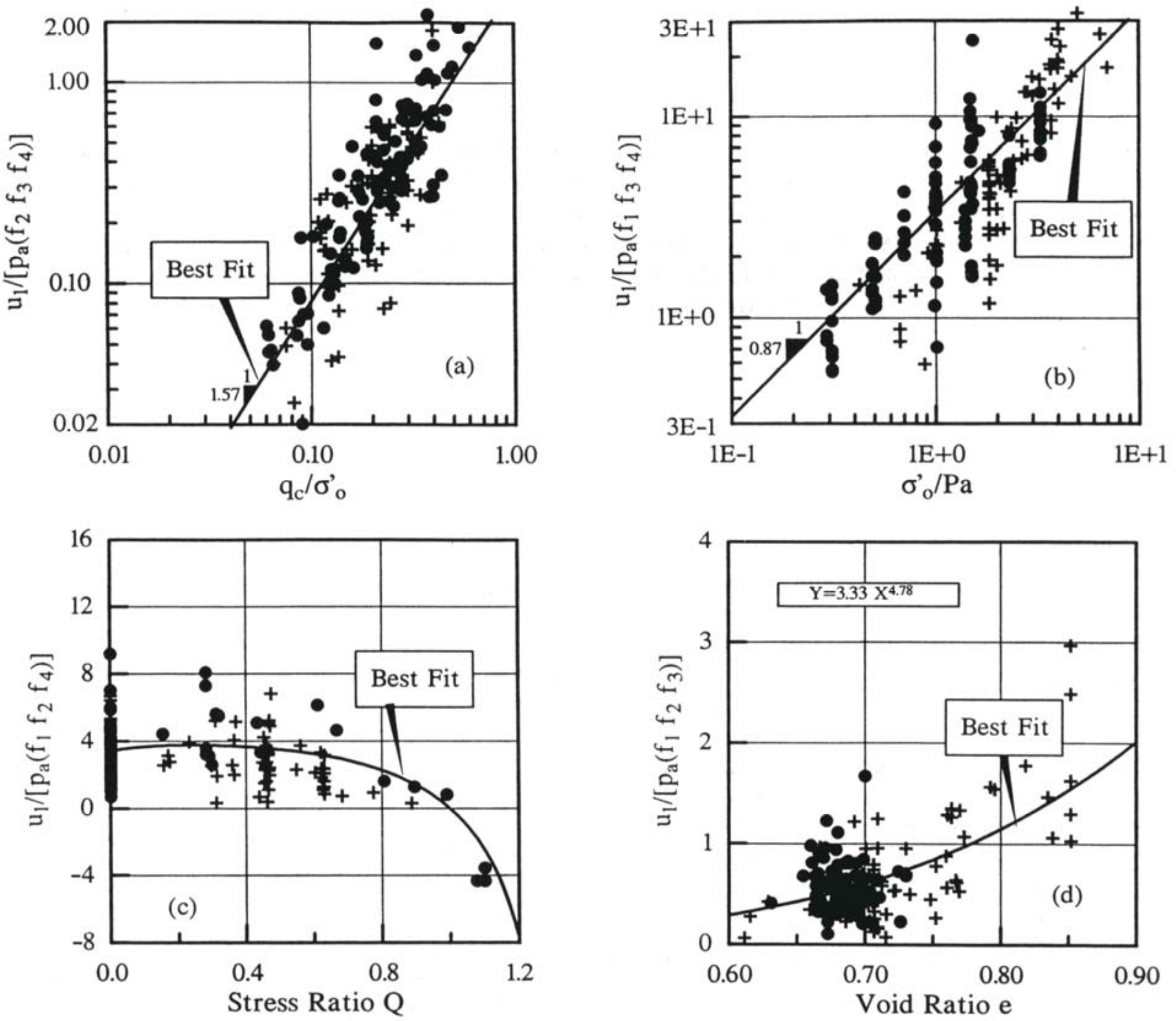

Figure 2. Comparison between analytical predictions and experimental data for excess pore pressures (● for NTUA sand & + for Oosterschelde sand).

simplified computations, the proposed relations provide reference for the calibration of constitutive models and numerical codes aimed at the prediction of cyclic sand response.

2 EXPERIMENTAL DATA

The experiments used herein have been performed on two similar cohesionless materials:

- Oosterschelde fine sand, with average particle diameter d_{50}=0.17 mm and uniformity index C_u=1.40 (Lambe 1979).
- NTUA sand, a material commonly tested at our geotechnical laboratory, with d_{50}=0.25 mm and C_u=1.7.

Oosterschelde sand has been prepared by wet tamping to void ratios e = 0.61 - 0.85, corresponding to medium - low relative volume density. NTUA sand has been prepared in the same way, but to a more narrow range of void ratios, e = 0.63 - 0.73, corresponding to medium density. All tests were either isotropicaly or anisotropicaly consolidated in compression ($\sigma'_v \geq \sigma'_h$) and the cyclic stress amplitude ($\pm$ $\sigma_{v,c}$) was maintained constant throughout cyclic loading.

The range of the initial and the cyclic stresses applied to the tests are summarized in Table 1 in terms of the following invariant quantities:

$$\sigma'_o = (\sigma'_v + 2\sigma'_h)/3 \quad , \quad q_o = (\sigma'_v - \sigma'_h)/2$$

$$q_c = \sigma'_{v,c}/2 \quad , \quad Q = q_o/\sigma'_o M$$

where M denotes the slope of the Phase Transformation line, which marks the bound between contraction and dilation in the q_o- σ'_o stress space (e.g. Ishihara et al. 1975).

3 EXCESS PORE PRESSURE

Figure 1 shows the variation of excess pore pressure u with number of (uniform) loading cycles, for one isotropic ($q_o \neq 0$) and two anisotropic ($q_o \neq 0$) tests. It is observed that, regardless of the initial value of q_o, the initial excess pore pressure increase is linear in the double logarithm scale of the figure. At later stages, the isotropic tests shows an abrupt increase in the rate of pore pressure build up which leads to liquefaction ($u = \sigma'_o$). The anisotropic tests do not show that abrupt increase, but tend to stabilize at a maximum excess pore pressure (u_f) which becomes less as q_o becomes larger.

The data in Figure 1 may be described approximately by extending the well known relations proposed by Seed and Booker (1977) for isotropic tests:

$$u = (2/\pi)\sigma'_o \arcsin\left[(N/N_l)^{1/2a}\right] \leq u_f \quad (1)$$

In Equation 1, N_l denotes the number of cycles required for liquefaction under isotropic conditions (the actual σ'_o and q_c but q_o=0), the exponent α ranges between 0.4 and 2.5, and

$$u_f = \sigma'_o - q_o/M \quad (2)$$

is the maximum limiting value of excess pore pressure, corresponding to an effective stress state that lays upon the Phase Transformation line (i.e. Luong and Sidaner 1981, Bouckovalas et al. 1983).

Application of Equation 1 for N=1, shows that N_l can be expressed in terms of the excess pore pressure after the first load cycle u_1:

$$N_l = \left[\sin([\pi/2][u_1/\sigma'_o])\right]^{-2a} \quad (3)$$

Hence, Equation 1 is finally written as:

$$u = (2/\pi)\sigma'_o \arcsin\left[N^{1/2a} \sin\left[(\pi/2)(u_1/\sigma'_o)\right]\right] \leq u_f \quad (4)$$

Analytical predictions according to the above equation, with a=1.28, are plotted with dotted lines in Figure 1 to compare with the respective experimental data.

Previous analyses of excess pore pressure (e.g. Egglezos & Bouckovalas 1998) have shown that u_1 can be expressed in product form, as:

$$u_1 = Ap_a(q_c/\sigma'_o)^{a1}(\sigma'_o/p_a)^{a2}(1 - Q^{a3})e^{a4} \quad (5)$$

or

$$u_1 = Ap_a f_1(q_c/\sigma'_o) f_2(\sigma'_o/p_a) f_3(Q) f_4(e) \quad (6)$$

where p_a is the atmospheric pressure, used to define the units. The material constants in Equation 5 were estimated from a multi-variable regression analysis (StatSoft Inc., 1995) on results from a total of 177

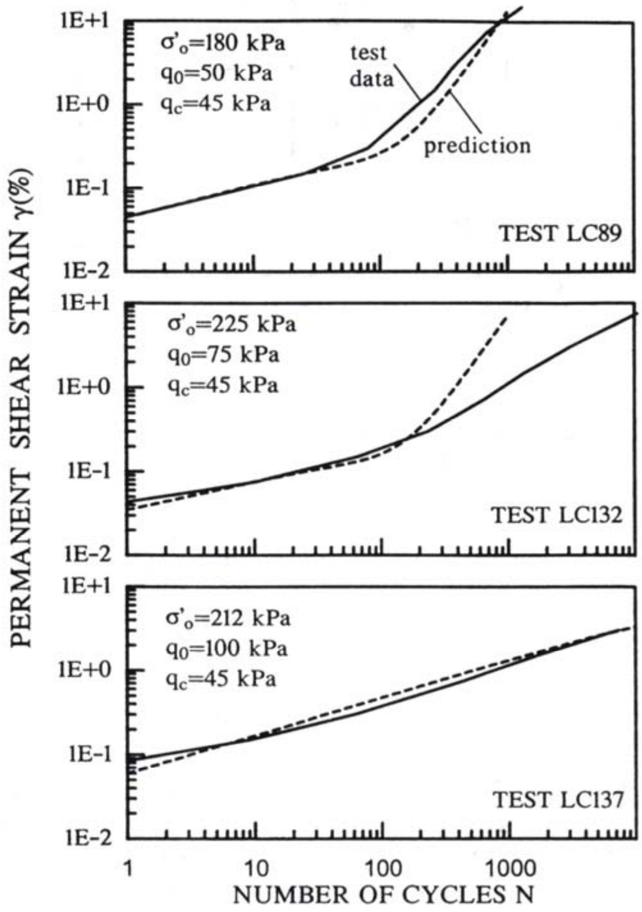

Figure 3. Typical experimental data for the variation of permanent shear strain with number of cycles (Oosterschelde sand).

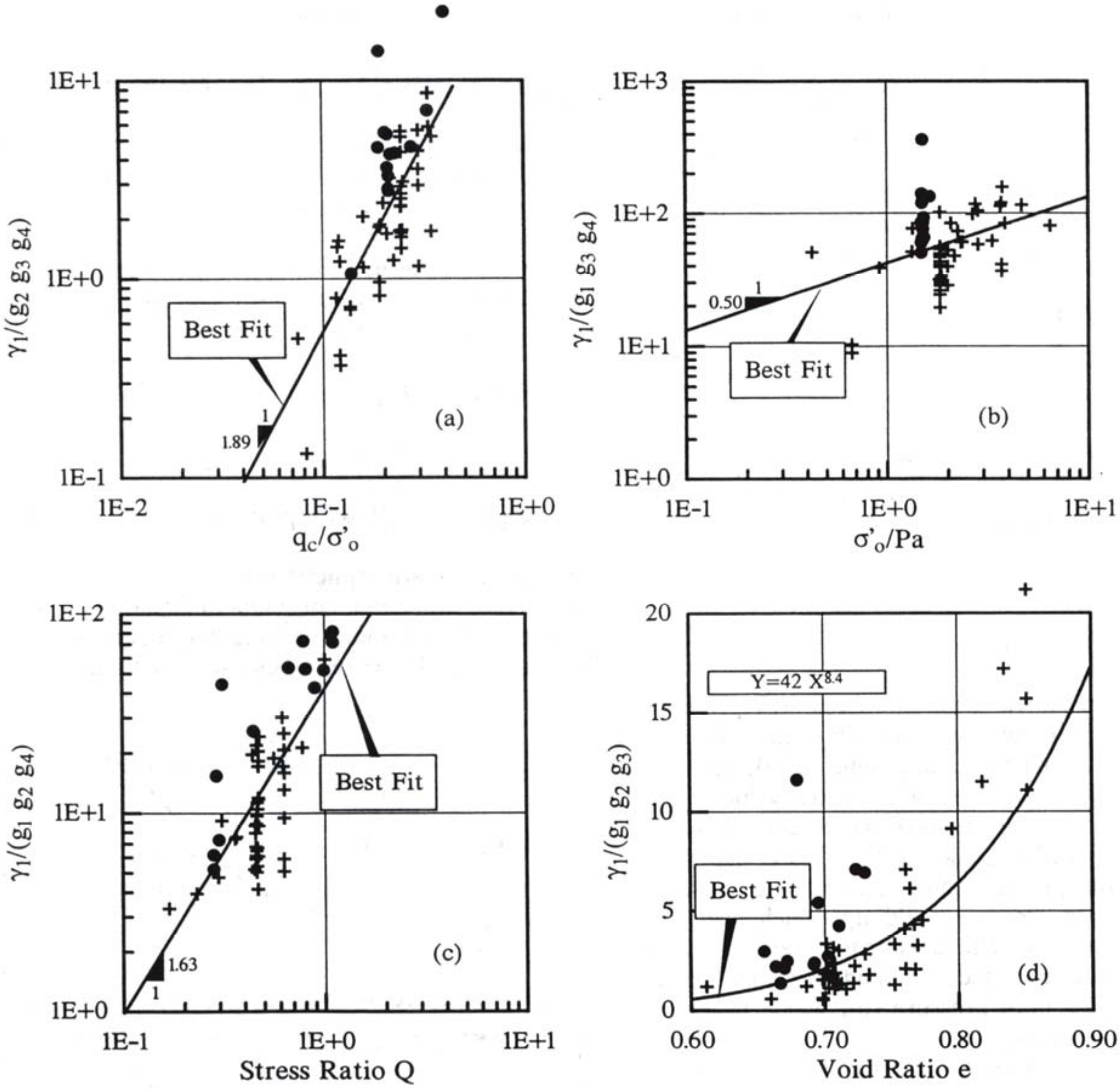

Figure 4. Comparison between analytical predictions and experimental data for permanent shear strain (● for NTUA sand & + for Oosterschelde sand).

tests. Thus, a reasonably good fit of the data (r=0.883) was obtained for:

A=4.00, a1=6.00, a2=1.00, a3=1.57 and a4=4.78

The effect of the various parameters on u_1 and the accuracy of the proposed relations are demonstrated in Figures 2a, 2b, 2c and 2d. Using an appropriate normalization of u_1, each figure focuses upon the effect of a single parameter. For instance, to focus upon the effect of the initial shear stress ratio, q_o/σ'_o has been plotted in Figure 2a against $u_1 / [p_a f_2(\sigma'_o/p_a) f_3(Q) f_4(e)]$.

4 PERMANENT SHEAR STRAIN

The variation of permanent shear strain γ (= ε_v - ε_h) with number of cycles N is depicted in Figure 3. In this case, experimental data are shown only for anisotropic tests as permanent shear strains for isotropic tests are negligible. Initially, the evolution of permanent strain is similar to that of excess pore pressure. Nevertheless, at the final stages of loading, excess pore pressures stabilize while permanent shear strains continue to accumulate at a relatively high rate. This variation is described analytically as:

$$\gamma = \gamma_1 N^{\beta}\left[1 - \left(N/N_{cr}\right) + 1.1\left(N/N_{cr}\right)^{1.25}\right] \quad (7)$$

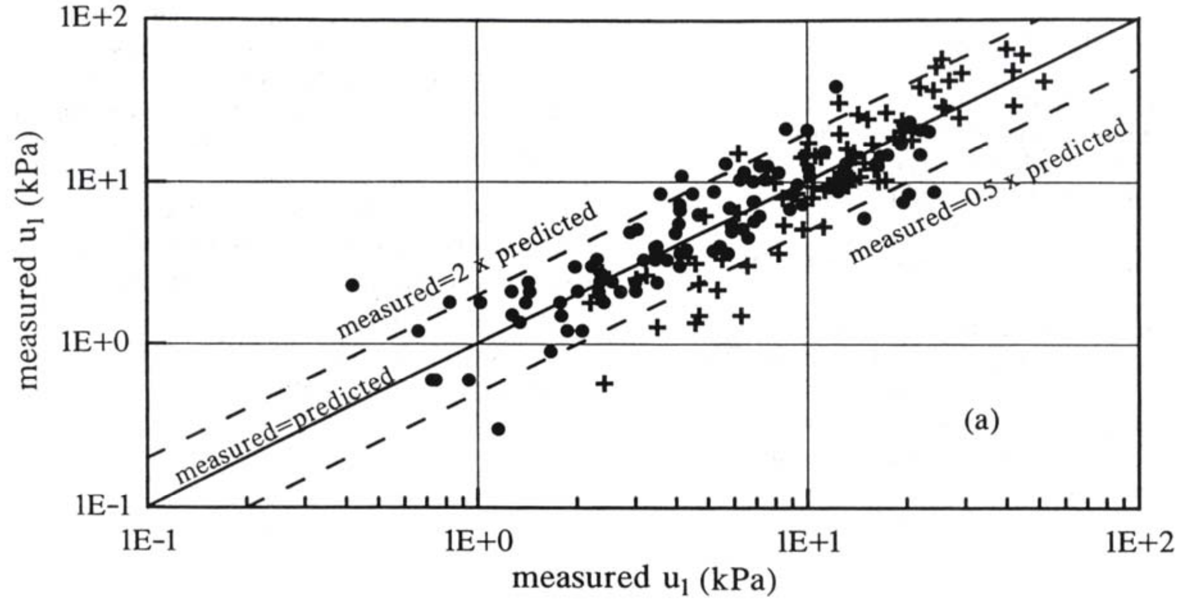

Figure 5. Predicted versus measured excess pore pressures at the end of the first loading cycle (● for NTUA sand & + for Oosterschelde sand).

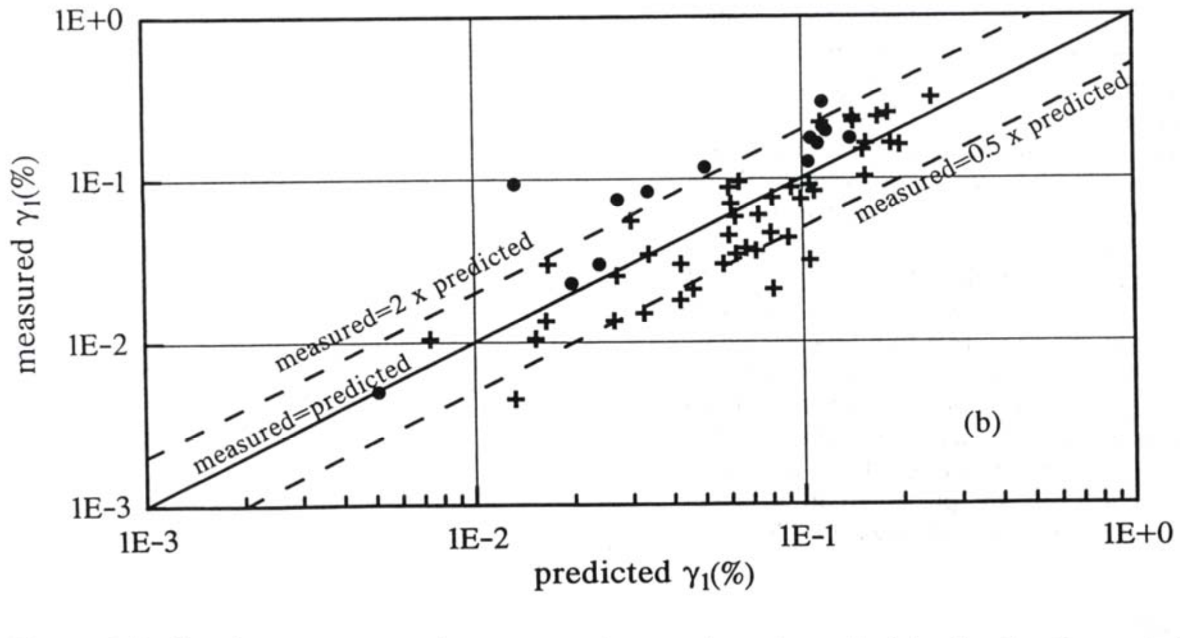

Figure 6. Predicted versus measured permanent shear strain at the end of the first loading cycle (● for NTUA sand & + for Oosterschelde sand).

where N_{cr} is the number of cycles where the curves in Figure 3 concave sharply upwards. Since this point corresponds grossly to the stabilization of excess pore pressures, N_{cr} may be computed approximately form Equation 4 assuming that $u(N_{cr})=u_f$. Thus:

$$N_{cr} = \left[\sin\left(\pi/2\, u_1/\sigma'_o\right) / \sin\left(\pi/2\, u_f/\sigma'_o\right)\right]^{2a} \tag{8}$$

According to the available experimental data, the exponent β in Equation 7 ranges between 0.15 and 0.90, with an average value of 0.44 (standard deviation of 0.20). Analytical predictions obtained with Equations 7 and 8 are plotted with dotted lines against the experimental data in Figure 3.

Permanent shear strain at the end of the first loading cycle γ_1 is expressed in the same general format as excess pore pressure u_1, i.e.:

$$\gamma_1(\%) = B\left(q_c/\sigma'_o\right)^{b1}\left(\sigma'_o/p_a\right)^{b2} Q^{b3} e^{b4} \tag{9}$$

or

$$\gamma_1(\%) = B g_1(q_c/\sigma'_o) g_2(\sigma'_o/p_a) g_3(Q) g_4(e) \qquad (10)$$

The material constants in Equation 9 were estimated from a multi-variable regression analysis on results from a total of 57 tests. Thus, a reasonably good fit of the data (r=0.813) was obtained for:

B= 42.0, b1=1.89, b2=0.50, b3=1.63 and b4=8.40

The analytical expression for γ_1 is compared to the experimental data in Figures 4a, 4b, 4c and 4d. The comparison is performed with the methodology adopted in Figure 2, for excess pore pressure u_1, i.e. separately for each of the independent variables entering Equations 9 and 10.

5 CONCLUSION

To evaluate the overall accuracy of the proposed relations, Figures 5 and 6 compare predicted to measured excess pore pressures u_1 and permanent shear strains γ_1. It is observed that analytical predictions are scattered, more or less symmetrically, around measurements, with the great majority of the data bounded between the lines corresponding to predicted-over-measured ratios of 0.5 and 2.0. Taking further into account that the scatter will increase at larger number of cycles, it is recommended that the proposed relations are used with a minimum factor of safety equal to 2.00.

It is important to clarify that the work presented herein applies strictly to medium-fine sands and stress-strain conditions consistent to undrained cyclic triaxial tests. The effects of soil type and test conditions are currently investigated with the aim to generalize the proposed relations. Preliminary results from this research, assessing these effects on excess pore pressure build up, are presented in a recent publication by Egglezos & Bouckovalas (1998).

REFERENCES

Bouckovalas G., R. V. Whitman & W. A. Marr 1983. Permanent displacement of sand with cyclic loading. *JGED, ASCE*, 100(11): 1606-1623.

Egglezos D. N. & G. Bouckovalas 1998. Analytical relationships for earthquake induced pore pressure in sand,clay and silt. *Proc. 11th European Conference on Earthquake Engineering, Paris, September* (in CD-ROM).

Ishihara K., F. Tatsuoka & S. Yashuda 1975. Undrained deformation and liquefaction of sand under cyclic stresses. *Soils and Foundations* 16(1): 1-16.

Lambe T. W. 1979. Cyclic triaxial tests on Oosterschelde sand. *MIT Research Report R79-24, Soils Publication No. 646.*

Luong M. P. & J. F. Sidaner 1981. Comportment cyclique et transitoiredes sables. *Proc. 10th ICSMFE, Stockholm, Sweden* 3: 257-260.

Seed H. B. & J. R. Booker 1977. Stabilization of potentially liquefiable sand deposits using gravel drains. *Journal of the Geotechnical Engineering Division, ASCE* 103(7): 757-768.

StatSoft, Inc. 1995. STATISTICA for windows [*computer program*]. Tulsa